SSRG International Journal of Mechanical Engineering
ISSN: 2348-8360/ https://doi.org/10.14445/23488360/IJME-V12I12P101

Volume 12 Issue 12, 1-9, December 2025
© 2025 Seventh Sense Research Group®

Original Article

Improving Drilled Hole Quality in Deep Hole Drilling of Stainless Steel Using Nanofluid Lubrication

Thu-Ha Mai[1], Van-Du Nguyen[2], Ky-Thanh Ho[3]

[1]*Thai Nguyen High School for Gifted Students, Thai Nguyen, Vietnam.*
[2]*Faculty of International Training, Thai Nguyen University of Technology, Thai Nguyen, Vietnam.*
[3]*Faculty of Mechanical Engineering, Thai Nguyen University of Technology, Thai Nguyen, Vietnam.*

[3]*Corresponding Author : hkythanh@tnut.edu.vn*

Received: 02 October 2025 Revised: 03 November 2025 Accepted: 05 December 2025 Published: 27 December 2025

Abstract *- This work presents a new lubrication strategy for single-stroke drilling of deep holes with a length-to-diameter ratio of eight in austenitic stainless steel SUS 304. The nanofluid used for cooling was prepared in two steps: initially, graphene nanosheets were dispersed into an emulsion, followed by dilution with tap water. All drilling trials were conducted at low pressure and flow rate, using internal lubrication through the drill bit. Compared with conventional emulsions, the nanofluid promoted more effective chip evacuation, lowered thrust force, and consequently prolonged tool life. The results further demonstrated that nanofluid lubrication in deep hole drilling enhanced hole quality, resulting in more uniform diameters and lower burr heights. Using a Taguchi L9 design, the optimal cutting parameters were determined as a spindle speed of 610 rpm and a feed rate of 0.06 mm/rev, which provided the best combination of dimensional accuracy and tool life. This strategy allows continuous deep-hole drilling without pecking, high-pressure coolant, or ultrasonic assistance, while remaining effective for difficult-to-cut materials.*

Keywords *- Nanofluid, Deep hole drilling, Chip morphology, Tool life, Diameter accuracy.*

1. Introduction

Drilling is a fundamental machining operation for producing holes in industrial components [1]. Because the cutting zone is deeply embedded within the workpiece, drilling is considered one of the most complex processes. Effective chip evacuation through the drill flutes is essential to prevent tool failure and maintain machining stability. These challenges are intensified in deep-hole drilling, particularly when the Length-to-Diameter (L/D) ratio exceeds five [2]. In such cases, chip evacuation becomes slower than chip generation, leading to chip clogging and a higher risk of tool failure.

The conventional flood lubrication approach is effective only when the L/D ratio remains below three [3]. In deep-hole drilling, insufficient lubrication and cooling hinder chip evacuation, leading to increased thrust force and drilling torque, and in severe cases, drill bit breakage [4].

Poor chip evacuation further reduces hole accuracy, degrades surface quality, and shortens tool life. Moreover, inadequate lubricant supply elevates cutting temperatures and promotes adhesion on the tool surface, thereby intensifying chip clogging. SUS 304 is a typical austenitic stainless steel, valued for its strength, ductility, toughness, and resistance to corrosion and oxidation [5]. It is widely applied in automotive, aerospace, medical, food, and chemical industries [6]. However, machining SUS 304 remains challenging due to its low thermal conductivity and strong tendency for work hardening, which leads to high cutting forces, elevated cutting temperatures, accelerated tool wear, and dimensional deviations in hole diameter [7]. Its high ductility further promotes the formation of long chips that entangle the drill bit, scratch the hole surface, and degrade hole quality [8]. These difficulties are intensified in deep-hole drilling, where chip evacuation is restricted, and process stability becomes harder to maintain.

Several approaches have been explored to enhance deep-hole drilling performance in SUS 304. Tool surface treatment and coating of tools [7], cryogenic cooling [9, 10], and optimization of drill bit geometry [8, 11] have shown benefits, though they are generally limited to holes with an L/D ratio below five. Peck drilling is often commended to improve chip evacuation and reduce work hardening in SUS 304 [12-14]. Nevertheless, this approach extends machining time and requires CNC automation. High-pressure internal cooling (about 60 bar) has been reported to enhance chip evacuation, thermal control, and surface finish in deep drilling of SUS 304 [15]. However, its adoption is restricted by high energy

This is an open access article under the CC BY-NC-ND license (http://creativecommons.org/licenses/by-nc-nd/4.0/)

demand and equipment costs. Ultrasonic-Assisted Drilling (UAD) promotes chip fragmentation, prevents chip adhesion, and improves lubrication, thereby reducing thrust force and torque and enabling deep-hole drilling of SUS 304 with an L/D ratio of up to eight. Yet, UAD requires precise resonance tuning for each tool geometry, raising implementation costs and limiting flexibility in mass production. Minimum Quantity Lubrication (MQL) is another method applied in drilling, reducing fluid consumption while maintaining effective cooling and lubrication at the cutting zone. Nevertheless, external MQL during drilling of SUS 304 is only effective when the L/D ratio is less than three [16]. Meanwhile, internal MQL is only effective when the supply pressure reaches at least 5 bar for holes with higher-than-five L/D ratios [17].

In recent years, nanofluids have attracted growing interest as advanced cutting fluids due to their enhanced thermal conductivity and tribological performance [18, 19]. The dispersed nanoparticles form a protective layer at the interface of the tool and chip, reducing friction and tool wear during machining. Their high thermal conductivity also facilitates efficient heat dissipation, stabilizes cutting temperatures, and enhances machining surface quality. However, when drilling AISI 321 stainless steel using external MQL, nanofluids have been shown to achieve an L/D ratio of 3.75 [20-22]. Several previous studies employed higher MQL flow rates, commonly referred to as Reduced Quantity Lubrication (RQL), typically ranging from 1000 mL/h to 30 L/h, much lower than conventional flood cooling, which often reaches about 720 L/h [23]. Nonetheless, this approach has only been applied to shallow hole drilling in stainless steel [23, 24] or titanium alloys [25].

For deep-hole drilling, a water-compatible nanofluid is made by dispersing graphene into an emulsion and diluting it with tap water. The nanofluid was supplied directly to the cutting zone through internal coolant channels at a pressure of 1.5 bar and a flow rate of 0.25 L/min. However, the stationary drill configuration used in these experiments does not represent typical industrial practice, where rotating drills are predominant.

This work presents experiments evaluating nanofluid lubrication for single-stroke deep drilling using RQL internal cooling and a rotating drill configuration, excluding pecking cycles, ultrasonic vibration, and high-pressure assistance. Experiments employed a 5 mm-diameter twist drill with an L/D ratio of eight on SUS 304. Drilling performance was compared between conventional lubrication and nanofluid, with emphasis on chip morphology, thrust force, tool life, and hole quality. Results showed that nanofluid reduced thrust force, extended tool life, and improved dimensional accuracy under RQL conditions. These benefits demonstrate the potential of nanofluids as a cost-effective approach to sustainable machining.

2. Materials and Methods

2.1. Experiment Setup

Figure 1 shows the experimental configuration. The tests employed a 5 mm-diameter twist drill (AQUA DEXOH8D, Nachi Inc., Japan) equipped with dual internal coolant channels to enhance chip evacuation and cooling. The drill features a flute length of 55 mm and a point angle of 135°. All experiments were performed on a 2UMB milling machine (Niigata Inc., Japan).

As illustrated in Figure 1, the twist drill bit (1) was mounted in a hollow collet (5), held securely by the machine spindle (7). A reCool system (6) from RegoFix Inc. directed lubricant through the collet into the drill's internal cooling passages. Coolant was supplied by a small pump (9), adapted from an automotive windshield washer unit, operating at 1.5 bar and 0.25 L/min via a connecting tube (8). The pump operated on a 12 VDC power source with a consumption of 24 W. The workpiece (2) was clamped in a jig (11) mounted on a Kistler 9257B tri-axial force sensor (4) to measure thrust forces. Figure 1(b) illustrates coolant delivery through the drill channels, while Figure 1(c) depicts the operating principle of the reCool system.

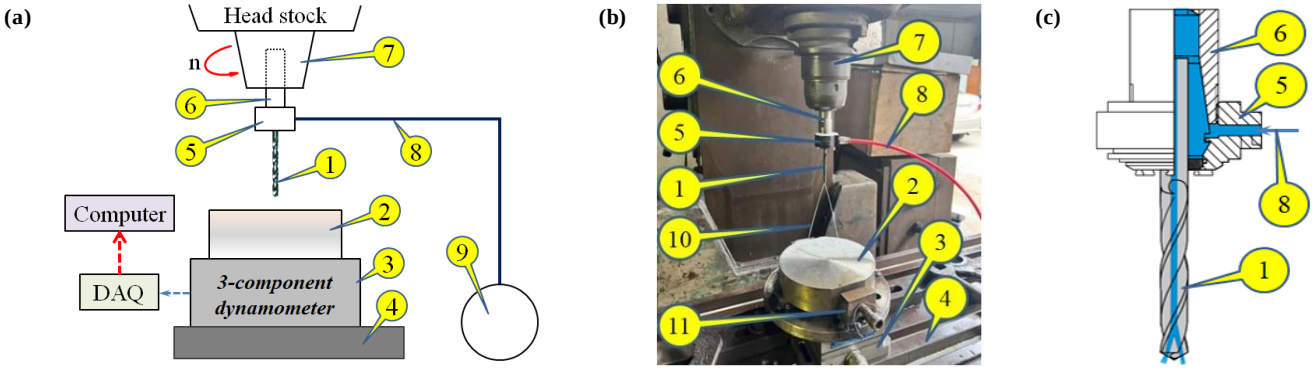

Fig. 1 The experimental setup, (a) Schematic arrangement, (b) Actual implementation captured in a photograph, and (c) Operational principle of the reCool system.

2.2. Preparing Material and Lubricant Fluid

For the experimental trials, commercially sourced SUS 304 bars with a diameter of 150 mm were selected. The 40-mm height specimens were prepared using Electrical Discharge Machining (EDM) wire-cutting. Throughout the drilling process, the tool penetrated the full height of the specimen, resulting in an L/D ratio of eight.

Two types of coolant fluids were utilized in this research: a nanofluid and a conventional emulsion. Both of them were water-based. Graphene nanosheets synthesized via a plasma-assisted technique, as detailed in reference [26], were used as a functional additive to formulate the nanofluid. Their morphology was characterized using Transmission Electron Microscopy (TEM, JEM-2100F, JEOL, Japan), revealing an average thickness of 2–10 nm and lateral dimensions of 1–4 μm. With a thermal conductivity approaching 3000 W/m.K, graphene offers far superior heat transfer compared to SUS 304. Although hydrophobic and poorly soluble in water, graphene can be effectively dispersed in emulsified systems [27]. For this work, Caltex Aquatex 3180—commonly used as a machining coolant and lubricant—was selected as the emulsifying agent.

Nanofluid preparation followed a two-step process, as outlined. In the first step, graphene nanosheets were dispersed into the emulsion serving as the carrier fluid. Due to their poor solubility in the emulsion, an ultrasonic horn was employed to achieve effective dispersion. The ultrasonic dispersion process was carried out at a frequency of 20 kHz for 30 minutes. The graphene nanosheets were blended with the emulsion at a concentration of 0.1 wt.%, corresponding to 100 mg of graphene dispersed in 100 mL of emulsion. For convenience, this mixture is referred to as emulsion-0.1 wt.% nano. In the second step, the prepared emulsion-0.1 wt.% nano was diluted with tap water to form the nanofluid. Following the manufacturer's, a typical composition of 10 vol.% (emulsion-0.1wt.% nano) and 90 vol.% tap water was adopted for this work.

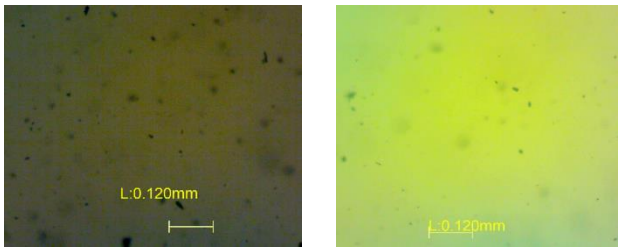

(a) **(b)**

Fig. 2 Optical microscopy, (a) The emulsion-0.1 wt.% nano mixture, and (b) The nanofluid, captured 24 hours after preparation.

After preparation, both the emulsion-0.1 wt.% nano mixture and the nanofluid were stored for 24 hours to evaluate their stability. As depicted in Figure 2(a), the graphene nanosheets (black spots) are well dispersed within the emulsion medium (dark background). In the nanofluid, as shown in Figure 2(b), the graphene nanosheets (brownish spots) exhibit a uniform distribution within the lighter aqueous phase containing dissolved emulsion. These observations indicate that graphene nanosheets are uniformly distributed in the base fluid, with no signs of agglomeration after 24 hours of preparation.

Besides the nanofluid, another coolant fluid, referred to as the conventional emulsion, was used for comparison. In this work, the conventional emulsion comprised 90 vol.% tap water and 10 vol.% emulsion. After preparation, both the nanofluid and the conventional emulsion were left to stabilize for 24 h before viscosity measurements. Viscosities of both fluids were measured with an NDJ-8S rotational viscometer. Tests were performed at room temperature and a spindle speed of 60 rpm. The nanofluid displayed a relative viscosity of 1.35 compared with tap water, while the conventional emulsion measured only 1.20.

2.3. Experiment Design

This study employed a four-phase experimental design. In the first phase, preliminary tests compared conventional emulsion and nanofluid lubrication, using hole completion as an indicator of drilling capacity. The second phase examined the effects of lubricant type on chip morphology, thrust force, and hole quality, with hole diameter differences assessed by a two-sample t-test. Phase three applied a Taguchi design to identify optimal cutting parameters for nanofluid drilling. The final phase validated these parameters and included a detailed analysis of the mean hole diameter and its distribution under both lubrication conditions.

All drilling trials used internal coolant delivery through the drill bit channels, maintained at a low pressure of 1.5 bar and a flow rate of 0.25 L/min. Nanofluid performance was benchmarked against conventional emulsion in terms of hole completion, chip morphology, thrust force, and hole quality. Although the manufacturer recommends peck drilling with incremental feeds of 0.2D–1.0D for SUS 304 when L/D exceeds five [14], this work adopted more demanding conditions: continuous through-hole drilling at L/D = 8 without pecking. A new drill bit was used for each trial, and cutting parameters followed manufacturer guidelines and prior studies.

3. Results and Discussion

3.1. Preliminary Tests

The preliminary findings are summarized in Table 1. As shown in Table 1, the first lubricant, conventional emulsion, was only capable of completing hole drilling at the lowest feed rate of 0.06 mm/rev, regardless of spindle speed. Even at this feed rate, successful hole formation occurred solely at spindle speeds of 430 rpm and 610 rpm. At a feed rate of 0.10 mm/rev, the emulsion fluid failed, causing tool breakage during the first

hole. In contrast, the nanofluid allowed complete drilling across all tested feed–speed combinations. The inclusion of graphene nanosheets clearly improved lubrication under demanding cutting conditions.

Table 1. Experiment settings and drilling ability of two lubricant types

No	Cutting Parameters		Types of Fluid	
	Spindle speed (rpm)	Feed rate (mm/rev)	Emulsion fluid (FE)	Nanofluid (NF)
1	430	0.04	✓	✓
2	610		✓	✓
3	870		✓	✓
4	430	0.06	✓	✓
5	610		✓	✓
6	870		×	✓
7	430	0.10	×	✓
8	610		×	✓
9	870		×	✓

3.2. Effect of Lubrication Fluids on Chip Morphology, Thrust Force, and Hole Quality

Figure 3 and Figure 4, respectively, present representative images of the post-drilling images under two different lubrication conditions, conventional emulsion and nanofluid, for comparative analysis of chip morphology and surface characteristics.

As shown clearly in Figure 3(b), the chips formed during drilling under conventional emulsion lubrication exhibit significant variation: initially appearing as short curls, then fragmenting into small pieces, becoming crushed and adhering to the drill flute (as depicted in Figure 3(a). This clogging is the main cause of incomplete machining under high cutting conditions with conventional emulsion, as shown in Table 1. Figure 3(c) and Figure 3(d) show that chips produced under conventional emulsion lubrication display serrated profiles, a typical feature when machining materials of low thermal conductivity under inadequate lubrication and heat dissipation [28]. Poor evacuation is also visible on the contact surface (Figure 3(d)), with alternating wave peaks and valleys. By contrast, chips generated with nanofluid lubrication (see Figure 4(b)) fracture at greater lengths, which promotes evacuation from the cutting zone and reduces adhesion or accumulation in the flutes (see Figure 4(a)). In addition, chips formed under nanofluid conditions (see Figure 4(c) and Figure 4(d)) present smoother surfaces and fewer serrations, reflecting improved removal efficiency and lower clogging risk during deep-hole drilling. These results can be attributed to the superior lubrication and cooling capacity of the nanofluid compared with conventional emulsions. Its higher viscosity lowers friction at the chip–tool–workpiece interfaces, thereby facilitating chip evacuation. In addition, the enhanced cooling reduces cutting temperature in the machining zone [18], leading to less chip deformation [28], more favorable fracture length, and easier removal.

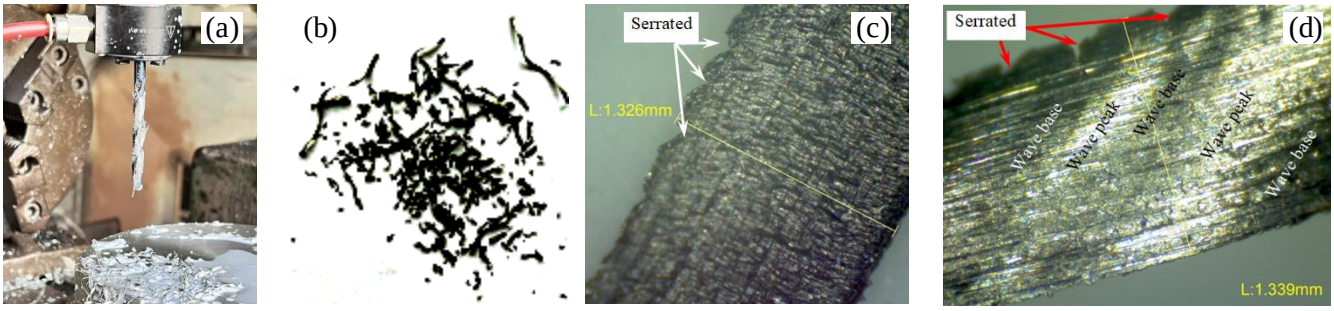

Fig. 3 (a) Drill bit after retraction, (b) Chip morphology, (c) Chip free surface, and (d) Chip contact surface, observed when drilling under conventional emulsion lubrication.

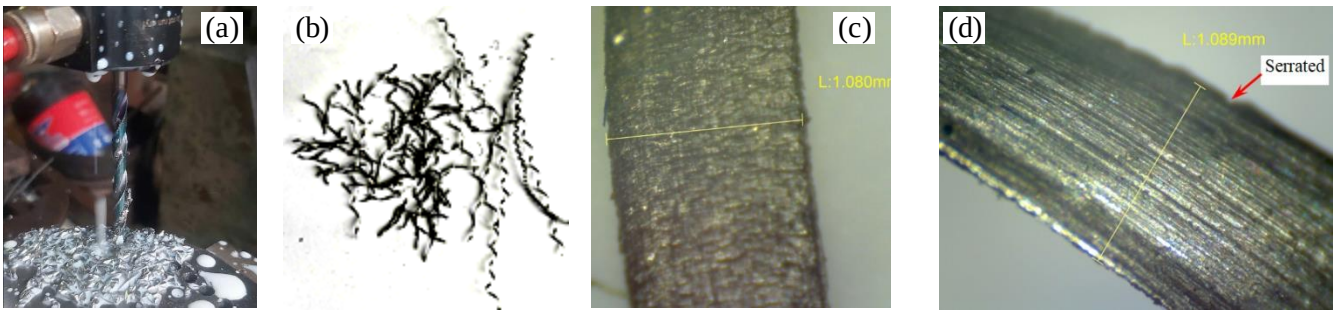

Fig. 4 (a) Drill bit after retraction, (b) Chip morphology, (c) chip free surface, and (d) Chip contact surface, observed when drilling under nanofluid lubrication.

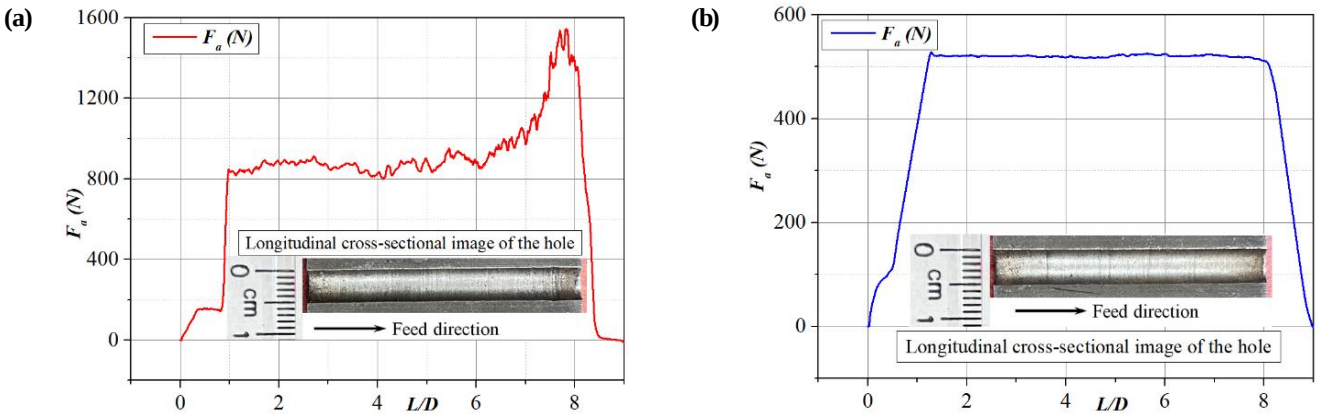

Fig. 5 Thrust force diagrams and longitudinal cross-sectional images of the holes obtained under different drilling conditions, (a) Using emulsion fluid, spindle speed of 430 rpm & feed rate of 0.04 mm/rev, and (b) Using nanofluid, spindle speed of 610 rpm & feed rate of 0.06 mm/rev.

Figure 5 presents the cutting force diagrams obtained under different drilling conditions. Under conventional emulsion lubrication, it can be seen that there is a high thrust force with significant fluctuation because of poor chip evacuation capability (see Figure 5(a)). Additionally, chip jamming occurred, resulting in a sudden jump in thrust force near the end of the drilling stroke. As a consequence of poor chip evacuation and chip jamming, the hole surface becomes scratched, and the hole diameter is enlarged.

In contrast, the thrust force obtained when drilling with nanofluid (see Figure 5(b)) is lower and more stable than that with conventional emulsion. Besides, the obtained hole surface under nanofluid lubrication is also smoother. These results further confirm the effectiveness of nanofluid in improving chip evacuation and heat dissipation conditions during deep hole drilling of difficult-to-machine materials.

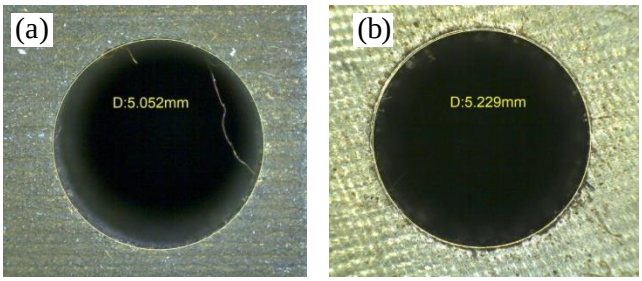

Fig. 6 Entrance hole diameters obtained with different lubricants, (a) Nanofluid, and (b) Conventional emulsion.

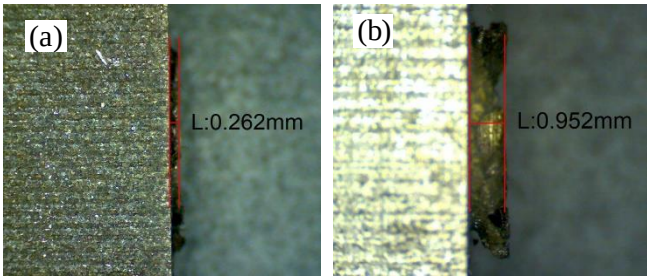

Fig. 7 Burr height obtained with different lubricants, (a) Nanofluid, and (b) Conventional emulsion.

Effective chip evacuation during drilling with nanofluid lubrication not only reduces thrust force but also contributes to improved hole quality. As shown in Figure 6, the hole diameter at the entrance obtained under nanofluid lubrication (see Figure 6(a)) is significantly smaller than that obtained under conventional emulsion lubrication (see Figure 6(b)).

Clearly, the reduction in thrust force and effective chip evacuation contribute to minimizing deviations in hole diameter. Moreover, the burr height at the exit of the drilled hole using nanofluid lubrication (see Figure 7(a)) is also significantly lower than that obtained using conventional emulsion lubrication (see Figure 7(b)). Lower burr height reduces post-processing time, thereby improving overall machining efficiency.

The subsequent section will present a comparative analysis of the effectiveness of nanofluid versus conventional emulsion in minimizing hole diameter.

3.3. Influence of Lubricants on the Hole Diameter

To evaluate the performance differences between nanofluid and conventional emulsion, a two-sample t-test was employed to analyse the statistical significance between the two groups. Drawing from the experimental data, the test revealed significant distinctions. For this comparative evaluation, the hole diameter, measured for each drilled hole under both lubrication conditions, was selected as the primary indicator.

The results are illustrated in Figure 8, and detailed data are presented in Table 2. Figure 8 indicates that the average hole diameter obtained using nanofluid is markedly lower than that obtained using conventional emulsion. Moreover, the variation in hole diameter obtained using nanofluid is also smaller than that observed with conventional emulsion. Furthermore, the detailed data in Table 2 show that nanofluid lubrication results in both a lower mean and standard deviation of hole diameter compared to conventional emulsion.

Table 2. Detailed results of the two-sample t-test

Factor	Lubricant fluid	Mean	Standard deviation	SE Mean	Difference estimated	95% CI for difference	P-value
Diameter of hole, d	Emulsion fluid	5.2878	0.0823	0.027	0.2267	(0.1953, 0.2940)	0.000
	Nanofluid	5.0611	0.0408	0.014			

With all p-values which are much smaller than 0.05, it can be confirmed that the hole diameter using nanofluid is significantly smaller than that obtained using conventional emulsion. In addition, statistical inference with 95% confidence intervals, none of which include zero, indicates significant differences between the means of the two populations.

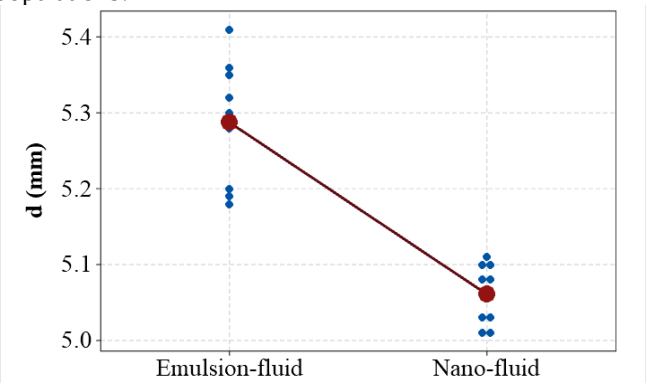

Fig. 8 Results of the two-sample t-test

3.4. Selection of Cutting Parameters

A Taguchi experimental approach was employed to determine optimal cutting parameters under nanofluid lubrication. This method utilizes orthogonal arrays to isolate the effects of individual factors, thereby significantly reducing experimental time and resource consumption. In this work, two control variables, each examined at three different levels, were selected, as outlined in Table 3.

Table 3. Experimental parameters and their levels

Cutting parameters	Levels		
	Low	Middle	High
Spindle speed *n* (rpm)	430	610	870
Feed rate *f* (mm/rev)	0.04	0.06	0.10

A standard L9 Taguchi design was implemented to optimize the drilling conditions. The response variable was defined as the minimum hole diameter obtained in each trial. Since the goal was to minimize this value, the smaller-is-better Signal-To-Noise (S/N) ratio criterion was adopted. Optimal factor levels were identified based on the lowest mean values observed.

Moreover, Taguchi methodology recommends maximizing the S/N ratio to improve process robustness against variability. The experimental outcomes are summarized in Table 4, while the main effects plots for minimum hole diameter (d) and corresponding S/N ratios are illustrated in Figure **9**.

Table 4. Experimental results of hole diameter d (mm)

Spindle speed *n* (rpm)	Feed rate *f* (mm/rev)	Hole diameter *d* (mm)			
		No.1	No.2	No.3	Average
430	0.04	5.09	5.12	5.12	5.11
430	0.06	5.03	5.02	5.04	5.03
430	0.10	5.09	5.11	5.10	5.10
610	0.04	5.08	5.08	5.07	5.08
610	0.06	5.02	5.01	5.01	5.01
610	0.10	5.04	5.03	5.02	5.03
870	0.04	5.10	5.11	5.10	5.10
870	0.06	5.02	5.01	5.01	5.01
870	0.10	5.07	5.08	5.08	5.08

As illustrated in Figure 9(a), the cutting parameter combination of spindle speed of 610 rpm and feed rate of 0.06 mm/rev resulted in the smallest hole diameter among all tested configurations. This finding is further supported by the highest Signal-To-Noise (S/N) ratio observed for the same parameter set, as shown in Figure 9(b), thereby reinforcing its optimality.

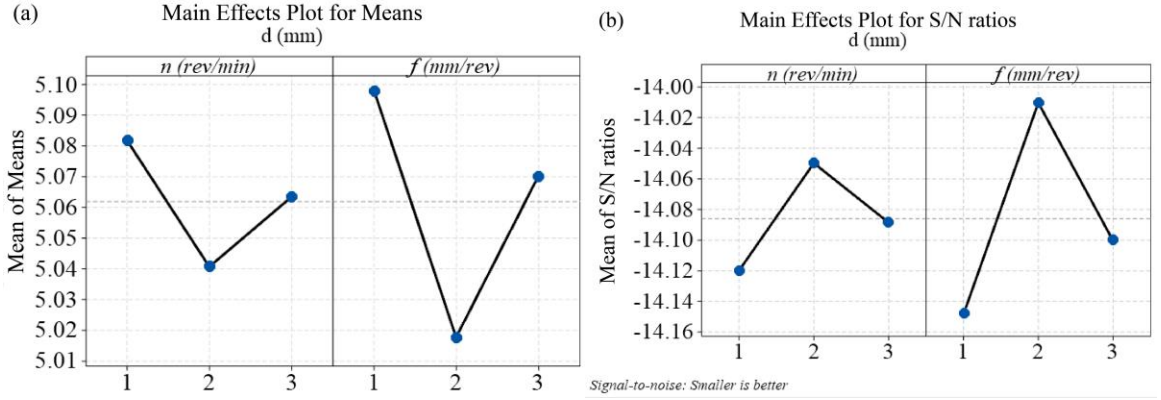

Fig. 9 Taguchi experimental results of (a) The mean values, and (b) The S/N ratios.

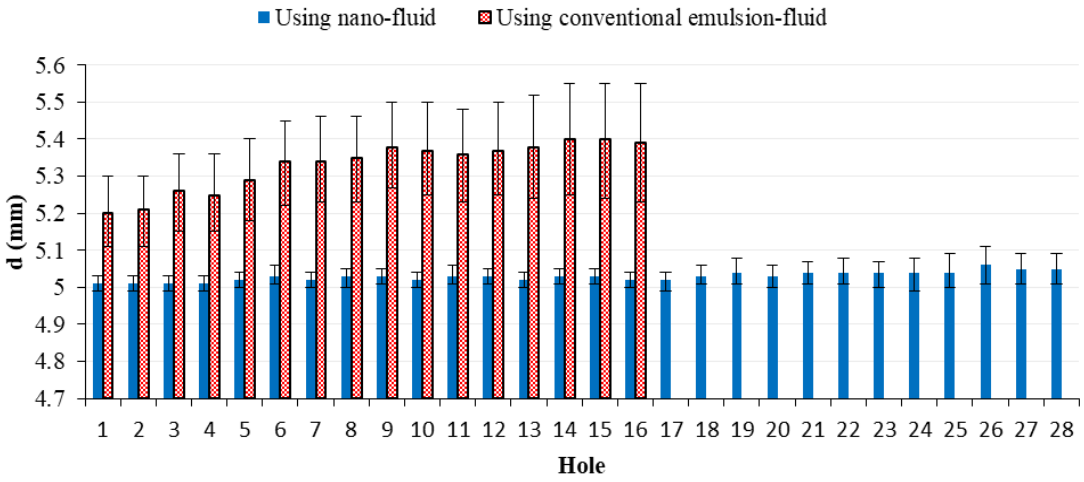

Fig. 10 Error bar chart showing the mean and variation of hole diameter for two types of lubricant under optimal cutting conditions

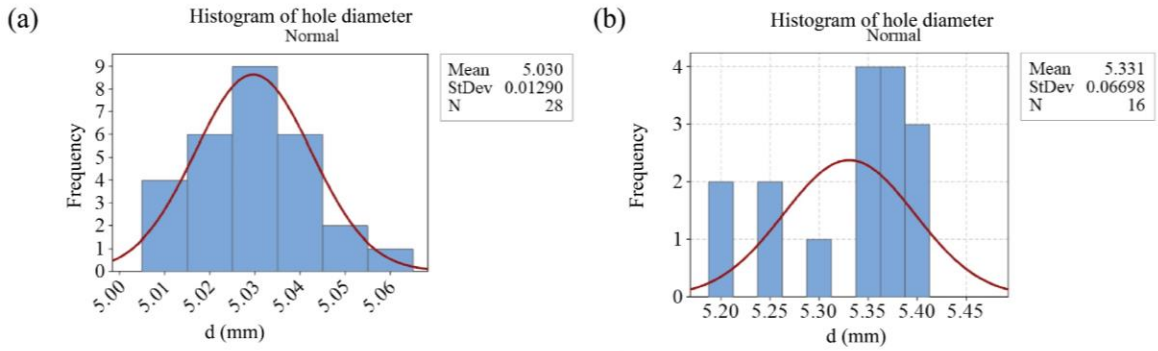

Fig. 11 Histogram of hole diameters obtained under optimal cutting conditions using, (a) Nanofluid, and (b) Conventional emulsion.

3.5. Validation Experiment

Following the Taguchi experimental analysis, a validation test was carried out using the identified optimal parameter set. A multi-hole drilling was conducted using nanofluid lubrication with the optimized cutting parameters: spindle speed of 610 rpm and feed rate of 0.06 mm/rev. In addition, a comparative experiment was conducted using the same cutting parameters but with a conventional emulsion to evaluate the beneficial effect of nanofluid lubrication. In this test, a brand-new drill bit was used for each type of lubricant. Under nanofluid lubrication, a new drill bit completed 28 holes without failure. In contrast, with a conventional emulsion, the bit fractured after only 16 holes. This outcome highlights the superior lubricating capacity of nanofluid and its contribution to longer tool life.

Figure 10 shows an error bar chart of hole diameters obtained with the two lubricants under optimized cutting parameters. Diameters were recorded at three positions in each hole: entrance (L/D = 0), middle (L/D = 4), and exit (L/D = 8). With nanofluid lubrication, the values ranged from 5.01 to 5.06 mm, which is markedly narrower than the 5.20–5.40 mm range observed with conventional emulsion. The chart also reveals a tendency for diameters to increase in successive holes, likely due to tool wear, which elevates thrust force and induces drill tip vibration. Besides, the diameter errors with the nanofluid were notably lower than those with the conventional emulsion.

Figure 11 compares the distribution of hole diameters obtained using two types of lubricant. The diameter distribution of the holes using nanofluid is narrower, with a mean diameter of 5.030 mm and a standard deviation of 0.01290 mm. In contrast, using conventional emulsion, the distribution is wider, with a mean diameter of 5.331 mm and a higher standard deviation of 0.06698 mm. The larger variance reflects reduced uniformity and greater fluctuations in hole diameters. Under nanofluid lubrication (see Figure 11(a)), the distribution is close to normal, consistent with a stable drilling process. In contrast, emulsion lubrication (see Figure 11(b)) produces a skewed distribution, pointing to instability during drilling.

Overall, compared to conventional emulsion, nanofluid lubrication improved chip evacuation, extended tool life, and yielded better hole quality. Moreover, these findings are particularly meaningful when machining hard-to-cut materials, where chip evacuation, as well as maintaining precision and stability during cutting, is often challenging. Besides, the results confirm that deep-hole drilling can be

performed continuously under RQL conditions with low pressure and low flow rate using nanofluid, eliminating the need for peck drilling, high-pressure coolant, or ultrasonic assistance. Compared to the stationary drill bit configuration, the rotating drill bit facilitates more effective chip breaking, thereby improving chip evacuation, reducing chip clogging, and prolonging tool life.

4. Conclusion

This work successfully developed and evaluated a new lubrication strategy capable of continuously drilling deep holes with a length-to-diameter ratio of eight, on SUS 304 austenitic stainless steel. Experimental results showed that under nanofluid lubrication, the obtained chips exhibited more suitable lengths and smoother surfaces, thereby evacuating more efficiently and preventing clogging compared to using conventional emulsion. As a result, the thrust force was reduced, and thus the tool life was extended. The results of the two-sample t-test revealed that hole diameter was more accurate and burr height was lower when drilling under nanofluid lubrication conditions. Under nanofluid conditions, the optimal cutting parameters were determined using the Taguchi method to be a spindle speed of 610 rpm and a feed rate of 0.06 mm/rev, which yielded the smallest hole diameter. Validation results further confirmed that the nanofluid contributed to improved tool life and hole diameter accuracy. These results demonstrate the great potential of the reduced quantity lubrication method using nanofluid in deep hole drilling of difficult-to-machine materials.

Future studies can apply reduced-quantity lubrication using other types of nanofluids to further expand the applicability of this lubrication method in deep-hole drilling.

Future research could explore the influence of different types and concentrations of nanoparticles on drilling performance, particularly in relation to chip morphology, thermal behavior, and tool wear behaviour. In addition, further research could explore the application of this lubrication solution to other difficult-to-machine materials without relying on alternative approaches such as peck drilling, high-pressure coolant, or ultrasonic assistance.

Acknowledgments

The authors would like to express their thanks to Thai Nguyen University of Technology, Thai Nguyen, Vietnam.

References

[1] Arshad Noor Siddiquee et al., "Optimization of Deep Drilling Process Parameters of AISI 321 Steel Using Taguchi Method," *Procedia Materials Science*, vol. 6, pp. 1217-1225, 2014. [CrossRef] [Google Scholar] [Publisher Link]

[2] Robert Heinemann et al., "The Performance of Small Diameter Twist Drills in Deep-Hole Drilling," *Journal of Manufacturing Science and Engineering*, vol. 128, no. 4, pp. 884-892, 2006. [CrossRef] [Google Scholar] [Publisher Link]

[3] Abdelkrem Eltaggaz, and Ibrahim Deiab, "Comparison of Between Direct and Peck Drilling for Large Aspect Ratio in Ti-6Al-4V Alloy," *The International Journal of Advanced Manufacturing Technology*, vol. 102, pp. 2797 - 2805, 2019. [CrossRef] [Google Scholar] [Publisher Link]

[4] Ce Han et al., "Chip Evacuation Force Modelling for Deep Hole Drilling with Twist Drills," *The International Journal of Advanced Manufacturing Technology*, vol. 98, pp. 3091-3103, 2018. [CrossRef] [Google Scholar] [Publisher Link]

[5] Amresh Kumar et al., "A Review on Machining Performance of AISI 304 Steel," *Materials Today: Proceedings*, vol. 56, pp. 2945-2951, 2022. [CrossRef] [Google Scholar] [Publisher Link]

[6] Bahman Azarhoushang et al., "The Effects of Alloy Composition and Surface Integrity on the Machinability of Austenitic Stainless Steels 304 and 304L," *Journal of Manufacturing and Materials Processing*, vol. 8, no. 6, pp. 1-17, 2024. [CrossRef] [Google Scholar] [Publisher Link]

[7] Sarmad Ali Khan et al., "Wear Performance of Surface Treated Drills in High Speed Drilling of AISI 304 Stainless Steel," *Journal of Manufacturing Processes*, vol. 58, pp. 223-235, 2020. [CrossRef] [Google Scholar] [Publisher Link]

[8] Josef Sedlak et al., "Effect of High-Speed Steel Screw Drill Geometry on Cutting Performance when Machining Austenitic Stainless Steel," *Scientific Reports*, vol. 13, pp. 1-13, 2023. [CrossRef] [Google Scholar] [Publisher Link]

[9] M. Arun et al., "Investigation on the Performance of Deep and Shallow Cryogenic Treated Tungsten Carbide Drills in Austenitic Stainless Steel," *Measurement*, vol. 125, pp. 687-693, 2018. [CrossRef] [Google Scholar] [Publisher Link]

[10] Vipin Pahuja et al., "Influence of Process Parameters on Surface Roughness Hole Diameter Error and Burr Height in Drilling of 304L Stainless Steel," *Conference Proceedings: Manufacturing Engineering*, pp. 117-135, 2019. [CrossRef] [Google Scholar] [Publisher Link]

[11] Lukáš Pelikán et al., "Novel Drill Geometries for Dry Drilling of Stainless Steel," *Journal of Manufacturing Processes*, vol. 92, pp. 500-520, 2023. [CrossRef] [Google Scholar] [Publisher Link]

[12] *Drilling Handbook: ISCAR's Reference Guide*, ISCAR, pp. 1-352, 2013. [Publisher Link]

[13] The Best Metalworking Videos, Practicalmachinist. [Online]. Available: https://www.practicalmachinist.com/

[14] Choosing the Right Pecking Cycle Approach, Harvey Performance Company, 2018. [Online]. Available: https://www.harveyperformance.com/in-the-loupe/choosing-the-right-pecking-cycle-approach/

[15] Asier Gandarias et al., "Study of the Performance of the Turning and Drilling of Austenitic Stainless Steels using Two Coolant Techniques," *International Journal of Machining and Machinability of Materials*, vol. 3, no. 1-2, pp. 1-17, 2008. [CrossRef] [Google Scholar] [Publisher Link]

[16] R. Heinemann et al., "Effect of MQL on the Tool Life of Small Twist Drills in Deep-hole Drilling," *International Journal of Machine Tools and Manufacture*, vol. 46, no. 1, pp. 1-6, 2006. [CrossRef] [Google Scholar] [Publisher Link]

[17] David A. Stephenson, Ethan Hughey, and Aleem A. Hasham, "Air Flow and Chip Removal in Minimum Quantity Lubrication Drilling," *Procedia Manufacturing*, vol. 34, pp. 335-342, 2019. [CrossRef] [Google Scholar] [Publisher Link]

[18] Shuguo Hu et al., "Nanoparticle-Enhanced Coolants in Machining: Mechanism, Application, and Prospects," *Frontiers of Mechanical Engineering*, vol. 18, no. 4, pp. 1-47, 2023. [CrossRef] [Google Scholar] [Publisher Link]

[19] Abhijit Bhowmik et al., "A Comprehensive Review on the Viability of Minimum Quantity Lubrication Technology for Machining Difficult-to-Cut Alloys," *AIP Advances*, vol. 15, no. 3, pp. 1-22, 2025. [CrossRef] [Google Scholar] [Publisher Link]

[20] Amrit Pal, Sukhpal Singh Chatha, and Hazoor Singh Sidhu, "Performance Evaluation of the Minimum Quantity Lubrication with Al_2O_3-Mixed Vegetable-Oil-Based Cutting Fluid in Drilling of AISI 321 Stainless Steel," *Journal of Manufacturing Processes*, vol. 66, pp. 238-249, 2021. [CrossRef] [Google Scholar] [Publisher Link]

[21] Amrit Pal, Sukhpal Singh Chatha, and Hazoor Singh Sidhu, "Experimental Investigation on the Performance of MQL Drilling of AISI 321 Stainless Steel using Nano-Graphene Enhanced Vegetable-Oil-Based Cutting Fluid," *Tribology International*, vol. 151, 2020. [CrossRef] [Google Scholar] [Publisher Link]

[22] Amrit Pal, Sukhpal Singh Chatha, and Hazoor Singh Sidhu, "Tribological Characteristics and Drilling Performance of Nano-MoS_2-Enhanced Vegetable Oil-Based Cutting Fluid using Eco-Friendly MQL Technique in Drilling of AISI 321 Stainless Steel," *Journal of the Brazilian Society of Mechanical Sciences and Engineering*, vol. 43, 2021. [CrossRef] [Google Scholar] [Publisher Link]

[23] B. Naveen Krishna, and D. Samuel Raj, "Improvement of Hole Quality and Process Characteristics by Adopting Reduced Quantity Lubrication in Drilling of Stainless Steel 304," *International Journal of Productivity and Quality Management*, vol. 22, no. 2, pp. 190-204, 2017. [CrossRef] [Google Scholar] [Publisher Link]

[24] B. Naveena et al., "Simplified MQL System for Drilling AISI 304 SS using Cryogenically Treated Drills," *Materials and Manufacturing Processes*, vol. 32, no. 15, pp. 1679-1684, 2017. [CrossRef] [Google Scholar] [Publisher Link]

[25] D. Samuel Raj, C. Jerome Arul Praveen, Aarthi S. Kumaran, "Studies on Cryogenic Treated Drills Under Nano-Fluid Based Reduced Quantity Lubrication Conditions for Machining Ti6Al4V," *Proceedings of the ASME 2018 International Mechanical Engineering Congress and Exposition*, Pittsburgh, Pennsylvania, USA, pp. 1-11, 2018. [CrossRef] [Google Scholar] [Publisher Link]

[26] Nguyen Van Truong et al., *Ultrasonic-Assisted Cathodic Plasma Electrolysis Approach for Producing of Graphene Nanosheets*, Sonochemical Reactions, InTech Open, 2019. [CrossRef] [Google Scholar] [Publisher Link]

[27] A.G.N. Sofiah et al., "Immense Impact from Small Particles: Review on Stability and Thermophysical Properties of Nanofluids," *Sustainable Energy Technologies and Assessments*, vol. 48, 2021. [CrossRef] [Google Scholar] [Publisher Link]

[28] H. Hegab et al., "On Machining of Ti-6Al-4V using Multi-Walled Carbon Nanotubes-based Nano-Fluid Under Minimum Quantity Lubrication," *The International Journal of Advanced Manufacturing Technology*, vol. 97, pp. 1593-1603, 2018. [CrossRef] [Google Scholar] [Publisher Link]